

# 000 BEYOND MULTI-TOKEN PREDICTION: PRETRAINING 001 LLMs WITH FUTURE SUMMARIES 002 003 004

005 **Anonymous authors**

006 Paper under double-blind review

## 007 008 ABSTRACT 009 010

011 Next-token prediction (NTP) has driven the success of large language models  
012 (LLMs), but it struggles with long-horizon reasoning, planning, and creative writing,  
013 with these limitations largely attributed to teacher-forced training. Multi-  
014 token prediction (MTP) partially mitigates these issues by predicting several fu-  
015 ture tokens at once, but it mostly captures short-range dependencies and offers  
016 limited improvement. We propose future summary prediction (FSP), which trains  
017 an auxiliary head to predict a compact representation of the long-term future, pre-  
018 serving information relevant for long-form generations. We explore two variants  
019 of FSP: *handcrafted summaries*, for example, a bag of words summary of the fu-  
020 ture of the sequence, and *learned summaries*, which use embeddings produced by  
021 a reverse language model trained from right to left. Large-scale pretraining exper-  
022 iments (3B and 8B-parameter models) demonstrate that FSP provides improve-  
023 ments over both NTP and MTP across math, reasoning, and coding benchmarks.  
024

## 025 1 INTRODUCTION 026

027 Early progress in large language models was primarily driven by massive scaling of both data and  
028 compute (Brown et al., 2020; Kaplan et al., 2020). However, the returns from this vanilla scaling  
029 approach are beginning to diminish as we encounter the “data wall” (Sutskever, 2024). This has  
030 renewed efforts toward algorithmic advances, including new architectures and pretraining objectives,  
031 that can extract more predictive signal from a fixed amount of training data.

032 Next-token prediction (NTP) with teacher forcing—training models by conditioning on ground-truth  
033 history when predicting the next token—is foundational to current pretraining methods. However,  
034 this approach introduces a train-inference mismatch known as exposure bias: during inference, the  
035 model must rely on its own outputs rather than the ground truth, leading to compounding errors and  
036 degraded long-range generation quality (Bengio et al., 2015). Moreover, teacher forcing can induce  
037 training-time shortcut learning as well, where the model exploits local cues from the ground-truth  
038 prefix instead of capturing true long-range dependencies (Bachmann & Nagarajan, 2024). These  
039 issues manifest most clearly in tasks demanding extended reasoning, narrative coherence, and open-  
040 ended creativity (Papalampidi et al., 2022; Nagarajan et al., 2025).

041 An appealing alternative to teacher forcing is teacherless training, where the model learns from its  
042 own generations rather than relying on ground-truth histories. However, this approach is compu-  
043 tationally intensive and challenging to parallelize. As a practical compromise, recent research has  
044 explored multi-token prediction (MTP) methods (Gloeckle et al., 2024), which train auxiliary heads  
045 to predict several future tokens simultaneously. MTP has demonstrated success in large-scale sys-  
046 tems such as DeepSeek-V3 (Liu et al., 2024) and Qwen-3 (Yang et al., 2025). In MTP, each time step  
047 augments the standard next-token prediction ( $x_{t+1}$ ) with auxiliary heads that predict additional fu-  
048 ture tokens (e.g.,  $x_{t+2}$  and beyond). However, these methods typically assume independence among  
049 the predicted tokens given the prefix, resulting in poor approximations of the true joint distribution  
050 over long future spans.

051 In this work, we propose a different approach: rather than predicting multiple future tokens individ-  
052 ually, we train a *single* auxiliary head to *predict a summary representation of the future sequence*. It  
053 aims to push as much information as possible about the future into a single target vector, while fil-  
tering out information that is inherently unpredictable and would only introduce noise. At each time

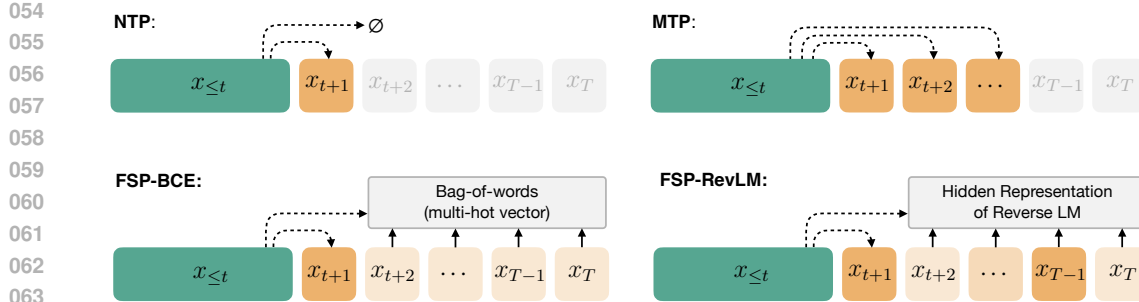


Figure 1: *A comparison of future-aware pretraining objectives.* All methods take a prefix  $x_{\leq t}$  as input. **NTP:** Only predicts the immediate next token. **MTP:** Uses multiple auxiliary heads, each predicting a specific future token. **FSP-BCE:** Our proposed hand-crafted summary method that predicts a multi-hot ‘bag-of-tokens’ summary of a long future window using a single auxiliary head. **FSP-RevLM:** Our proposed learned summary method predicts a compact hidden representation of the future, which is generated by a reverse language model (RevLM).

step  $t$ , given the future tokens  $(x_{t+2}, x_{t+3}, \dots, x_{t+\tau})$ , we construct a summary vector  $a(t, \tau)$  to provide supervision to the auxiliary head. We explore two complementary approaches for constructing future summaries: a simple token-level aggregation method, and our main contribution, a learned representation of the future sequence that captures long-range dependencies more effectively.

- **Hand-crafted summary.** We train the auxiliary head to predict *all* the future tokens that will occur in a future window, without requiring to know their exact positions. Concretely, at each step  $t$ , we define a multi-hot vector  $a(t, \tau)$  over the vocabulary, akin to bag-of-words, where  $a(t, \tau)_i = \mathbb{I}(i \in \{x_{t+2}, \dots, x_{t+\tau}\})$ , and train the model with a binary cross-entropy objective.
- **Learned summary.** Handcrafted summaries such as the one proposed above can be noisy: not all future tokens are equally relevant, and predicting them all can dilute the signal. To address this, we propose to *learn* a compact summary of the future. We do this by training a reverse language model ( $g_r$ ) on reversed sequences, so that its hidden representation  $a(t, \tau) = g_r(x_{\geq t+2})$  serves as a rich embedding of the future context. The auxiliary head of the forward model is then trained to match this representation with an  $\ell_2$  loss.

We use the lens of synthetic tasks, path-star graph and sibling discovery (Bachmann & Nagarajan, 2024; Nagarajan et al., 2025) to clarify the conceptual difference between MTP and our approach. On path-star graph, hand-crafted summaries deliver strong gains over MTP, which only predicts immediate future tokens, demonstrating the benefit of long-horizon supervision. However, in sibling discovery, where the future includes content unrelated to the current local sequence, handcrafted summaries struggle, as they treat all future tokens equally. In contrast, our learned summary vectors focus on the informative parts of the future and achieve consistent gains.

We then scale our approach to real-world pretraining at the 8B parameter level, conducting a systematic evaluation across six methods, including DeepSeek-MTP and multiple handcrafted summary variants. This scale and breadth of comparison is rare in the literature due to its high computational cost. Here, the proposed future summary prediction with learned summaries yields substantial improvements over NTP and MTP baselines, with gains of up to 5% on math and coding benchmarks that demand long-horizon reasoning and planning. These results demonstrate that future summary prediction is not only effective in controlled synthetic settings but also translates into meaningful gains for large-scale LLM training.

## 2 FUTURE-AWARE PRETRAINING

### 2.1 BACKGROUND ON NEXT-TOKEN AND MULTI-TOKEN PREDICTION

Let define a sequence of tokens as  $X = (X_1, X_2, \dots, X_T)$  sampled from a distribution  $\mathbb{P}_X$ , where each token is a discrete random variable supported on  $\{1, 2, \dots, V\}$ .

108 **Next-Token Prediction (NTP).** The standard next-token prediction objective is:  
 109

$$110 \quad L_{\text{NTP}}(X, P_\theta) = -\mathbb{E}_{x \sim \mathbb{P}_X} \left[ \sum_{t=1}^{T-1} \log P_\theta(x_{t+1} | x_{\leq t}) \right], \quad (1)$$

112 where  $P_\theta$  is the predictor, optimized via  
 113

$$114 \quad \theta^* = \arg \min_{\theta} L_{\text{NTP}}(X, P_\theta). \quad (2)$$

115 A typical parameterization is:  
 116

$$117 \quad P_\theta(x_{t+1} | x_{\leq t}) = \text{softmax} \left( f_u \circ f_h \circ f_s(x_{\leq t}) \right), \quad (3)$$

119 where  $f_s$  is the transformer backbone,  $f_h$  is a processing head, and  $f_u$  is the unembedding layer  
 120 (Figure 2).

121 **Multi-Token Prediction (MTP).** MTP aims to jointly predict multiple future tokens, as follows:  
 122

$$123 \quad L_{\text{MTP-Joint}}(X, P_\theta) = -\mathbb{E}_{x \sim \mathbb{P}_X} \left[ \sum_{t=1}^{T-1} \log P_\theta(x_{t+1}, \dots, x_{t+\tau} | x_{\leq t}) \right]. \quad (4)$$

126 Since modeling the exact joint distribution is intractable, a common simplification is to model the  
 127 marginal distribution of future tokens given the prefix (Gloeckle et al., 2024; Liu et al., 2024):

$$128 \quad L_{\text{MTP}}(X, P_\theta) = -\mathbb{E}_{x \sim \mathbb{P}_X} \left[ \sum_{t=1}^{T-1} \sum_{k=1}^{\tau} \mathbf{1}[t+k \leq T] \log P_\theta(x_{t+k} | x_{\leq t}) \right]. \quad (5)$$

131 Following Gloeckle et al. (2024), the predictor uses separate auxiliary heads for each  $k$ :  
 132

$$133 \quad P_\theta(x_{t+1} | x_{\leq t}) = \text{softmax} \left( f_u \circ f_h \circ f_s(x_{\leq t}) \right), \\ 134 \quad P_\theta(x_{t+k} | x_{\leq t}) = \text{softmax} \left( f_u \circ f'_{h_k} \circ f_s(x_{\leq t}) \right), \quad \forall k > 1, \quad (6)$$

136 where  $f'_{h_k}$  are auxiliary transformer blocks specialized for predicting future tokens  $x_{t+k}$ .  
 137

138 This design reduces teacher forcing by predicting  $x_{t+k}$  from  $x_{\leq t}$  only, rather than conditioning on  
 139 the full prefix  $x_{\leq t+k-1}$ . This is the key principle behind multi-token prediction, i.e., reduced teacher  
 140 forcing by requiring the model to predict a block of future tokens at each step.

141 We discuss other variants of MTP such as DeepSeek-MTP and random future token MTP (Thankaraj  
 142 et al., 2025) in Appendix A.  
 143

## 144 2.2 FUTURE SUMMARY PREDICTION (FSP)

146 In MTP, we use a set of auxiliary heads to predict a block of immediate future tokens. A key  
 147 limitation of this approach is that one does not know exactly where the informative signal in the  
 148 future sequence lies. Informative signals in future could occur far away in the sequence and be well  
 149 beyond the number of future tokens ( $k$ ) that MTP predicts. A trivial approach to overcome this  
 150 could be to predict all the future tokens. However, having one auxiliary head per future token is not  
 151 scalable, and limits the amount of future tokens we can utilize during training.

152 Towards this, we propose *Future Summary Prediction* (FSP), that predicts a compact summary of  
 153 the (long) future sequence rather than each token individually.

154 Let  $a(t, \tau)$  represent a summary of future tokens  $(x_{t+2}, \dots, x_{t+\tau})$ . The learning objective is:  
 155

$$156 \quad L_{\text{FSP}}(X, P_\theta) = L_{\text{NTP}}(X, P_\theta) + \mathbb{E}_{x \sim \mathbb{P}_X} \left[ l_a(A_\phi(x_{\leq t}), a(t, \tau)) \right], \quad (7)$$

157 where  $P_\theta$  is the next-token predictor,  $A_\phi$  is the summary predictor, and  $l_a$  is the loss between pre-  
 158 dicted and ground-truth summaries. The architecture is:

$$159 \quad P_\theta(x_{t+1} | x_{\leq t}) = \text{softmax} \left( f_u \circ f_h \circ f_s(x_{\leq t}) \right), \\ 160 \quad A_\phi(x_{\leq t}) = f'_{h_a} \circ f_s(x_{\leq t}). \quad (8)$$

162 Unlike MTP, FSP requires only a single auxiliary head  $f'_{h_a}$ , making it  
 163 more scalable.

164 The key question, then, is how to construct an effective future summary.  
 165 In this work, we investigate two approaches:

166 **(1) Hand-crafted future summaries.** We define a binary vector  
 167  $a(t, \tau) \in \mathbb{R}^V$  indicating whether token  $i$  appears in the future window:

$$170 \quad a(t, \tau)_i = \mathbb{I}(i \in \{x_{t+2}, \dots, x_{t+\tau}\}). \quad (9)$$

171 Given logits from  $A_\phi(x_{\leq t})$ , we minimize a reweighted binary cross-  
 172 entropy loss:

$$174 \quad l_a(A_\phi(x_{\leq t}), a(t, \tau)) = - \sum_{i=1}^V w(i) \left[ a_i \log \sigma(z_i) + (1-a_i) \log (1-\sigma(z_i)) \right] \quad (10)$$

177 where  $a_i = \mathbb{I}(i \in \{x_{t+2}, \dots, x_{t+\tau}\})$ ,  $z_i$  is the  $i$ -th logit of  $A_\phi(x_{\leq t})$ ,  
 178  $\sigma$  is the sigmoid, and  $w(i)$  reflects the importance of token  $i$  (e.g. term  
 179 frequency-inverse document frequency, tf-idf).

180 **(2) Learned future summaries.** Predicting every future token via  
 181 hand-crafted summaries as discussed above could be noisy. For exam-  
 182 ple, not all tokens in the future are informative and thus hand-crafted summaries that account for all  
 183 of them can be wasteful. Instead of predicting all the future tokens, we therefore propose to predict  
 184 a learned representation of the future tokens relevant to predicting the current token  $x_{t+1}$ . We learn  
 185 this representation via a reverse language model  $Q_\psi$ , (RevLM), trained on "right-to-left" sequences:

$$187 \quad L_{\text{RevLM}}(X, Q_\psi) = -\mathbb{E}_{x \sim \mathbb{P}_X} \left[ \sum_{t=1}^{T-1} \log Q_\psi(x_{t+1} \mid x_{\geq t+2}) \right]. \quad (11)$$

190 RevLM shares the same architecture, and we take its hidden state as the summary vector:

$$191 \quad a(t, T-t) = g_h \circ g_s(x_{\geq t+2}). \quad (12)$$

192 We then train  $A_\phi(x_{\leq t})$  to match this representation via the  $\ell_2$  loss:

$$194 \quad l_a(A_\phi(x_{\leq t}), a(t, T-t)) = \|A_\phi(x_{\leq t}) - g_h \circ g_s(x_{\geq t+2})\|_2^2. \quad (13)$$

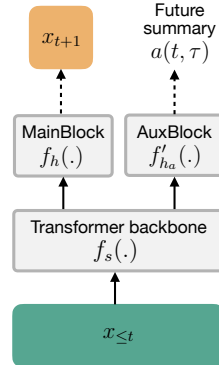
196 **Why Future Summary Prediction?** The key advantage of future summary prediction is its abil-  
 197 ity to reduce dependence on teacher forcing when modeling long future sequences. To intuitively  
 198 measure teacher forcing, consider for each ground-truth token exposed to the model, how much in-  
 199 formation is the model required to predict about unseen tokens? If the model predicts more such  
 200 information, then we have reduced teacher forcing. Next-token prediction (NTP) uses the highest  
 201 degree of teacher forcing, since the model always conditions on ground-truth histories to predict  
 202 just the next token. Multi-token prediction (MTP) partially relaxes this by asking the model to pre-  
 203 dict short blocks of future tokens, thereby reducing teacher forcing locally. However, MTP remains  
 204 constrained by the short horizon of its predictions. In contrast, our proposed approach predicts sum-  
 205 maries of long future sequences, substantially reducing teacher forcing by requiring the model to  
 206 reason about rich, global properties of the target trajectory.

### 207 3 ANALYZING FUTURE SUMMARIES

209 Future summary prediction provides a unified view of a broad family of pretraining objectives, cov-  
 210 ering MTP and its variants that sample random future tokens (Thankaraj et al., 2025; Gerontopoulos  
 211 et al., 2025), and our proposed bag-of-words (FSP-BCE) and reverseLM (FSP-RevLM) summary  
 212 prediction objectives.

213 To better understand how the FSP framework clarifies the tradeoffs of each objective on long-horizon  
 214 planning, we consider the graph modeling benchmarks introduced in prior works.

215 Our analysis yields following insights:

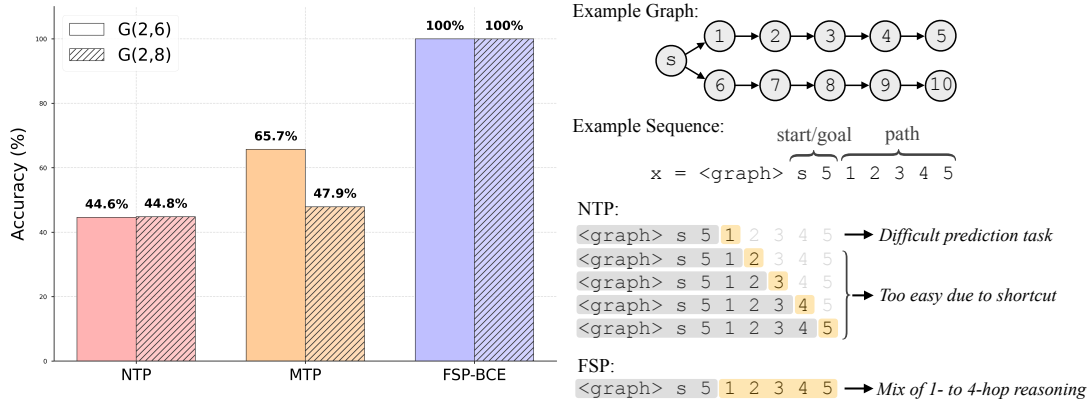


171 Figure 2: An abstraction  
 172 of the architecture that  
 173 subsumes NTP, MTP,  
 174 and FSP.

216

- 217 • **Long future summaries matter.** On the canonical path–star task (Bachmann & Nagarajan, 218 2024), we find that MTP with short range future prediction fails to generalize, highlighting 219 the need for auxiliary objectives that incorporate *long-range* future information.
- 220 • **Adaptive future summaries matter.** On a modified sibling discovery task (Nagarajan 221 et al., 2025), we show that incorporating every future token with hand-crafted summaries 222 is suboptimal, highlighting the need for *learned* summaries that retain key information.

223 3.1 LONG FUTURE SUMMARY IS IMPORTANT



239 Figure 3: *Analysis of FSP-BCE on the path-star task, which tests long-horizon planning.* **Left:** 240 Accuracy (mean over 5 random seeds) of different pretraining objectives on degree 2 graphs with 241 path lengths 6 and 8. Standard NTP generalizes poorly, and MTP’s accuracy degrades as the path 242 length increases, while FSP-BCE achieves perfect accuracy. **Right:** An illustration of why NTP fails 243 while FSP-BCE succeeds, where the input context is shown in `grey` and the target is in `beige`.

244 We consider the path-star graph, a directed acyclic graph (DAG)  $G(d, l)$  composed of  $d$  paths, each 245 of length  $l$ , originating from a central start node  $v_{\text{start}}$ . The model is provided with the adjacency list 246 of the graph in the prefix, and the task is to generate the path from  $v_{\text{start}}$  to a designated end node 247  $v_{\text{end}}$ .

248 Let the target path be  $(v_{\text{start}}, v_1, v_2, \dots, v_{\text{end}})$  and the input prefix be  $p = (\text{Adj}(G), v_{\text{start}}, v_{\text{end}})$ . Then 249 NTP with teacher forcing predicts an intermediate node in the path as  $P_\theta(v_{i+1}|p, v_{\leq i})$ . As shown 250 by Bachmann & Nagarajan (2024), NTP often learns shortcut solutions: the model can recover  $v_{i+1}$  251 directly from  $v_i$  by scanning the adjacency list in  $p$ , without learning the underlying long-range plan 252 (Figure 3). This leads to gradient starvation (Pezeshki et al., 2021), where the supervision signal 253 for the actual planning task is lost. Once the shortcut is learned, meaningful gradient information 254 remains only for predicting the first step  $v_1$ , as it is the only difficult token.

255 A natural remedy is to reduce teacher forcing via future prediction approaches, which require the 256 model to predict tokens further ahead. This makes shortcuts less effective, as multiple lookups in 257 the adjacency list would be needed to predict future tokens. Hence, we consider the MTP approach, 258 which predicts the immediate future token, and the handcrafted summary method FSP-BCE, which 259 compresses the information about all the future tokens from the path. By summarizing the entire 260 future trajectory, FSP-BCE substantially reduces teacher forcing, encouraging the model to plan the 261 full path instead of exploiting shortcuts.

262 We conduct experiments for two graphs  $G(2, 6)$  and  $G(2, 8)$ , with all the approaches pretrained 263 from scratch using the GPT-Mini architecture (details in Appendix B.1). At inference, we discard 264 the auxiliary head used in future prediction, and the task is to generate the complete path given the 265 prefix  $p$ . The evaluation metric checks whether the generated path exactly matches the true path. 266 Results in Figure 3 (left) show that both NTP and MTP fail to generalize (both obtained perfect 267 training accuracy), and the accuracy of MTP degrades further for the scenario with longer path 268  $G(2, 8)$ . Hence, predicting just the immediate future token is not enough, and FSP-BCE tackles this 269 by efficiently compressing all the future tokens from the path, enabling it to achieve perfect accuracy

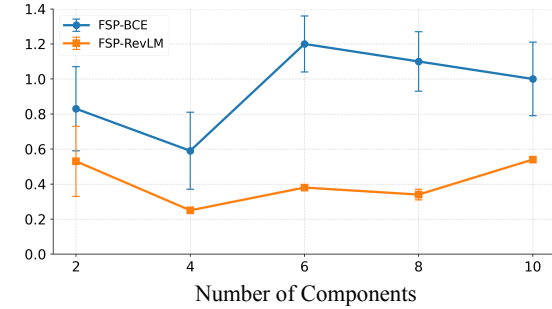
270 in both cases. Appendix B.1 (Table 4) shows that increasing the number of auxiliary heads in MTP  
 271 can provide some improvement, but practical limits exist: even with four additional future heads  
 272 MTP cannot solve the longer path graph  $G(2, 8)$ .  
 273  
 274

### 275 3.2 ADAPTIVE FUTURE SUMMARY IS IMPORTANT

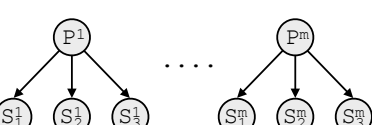
276

277

278 Convergence Speed Relative to NTP:



279 Graph:



280 Example Sequence:

281  $x = S_1^1 S_1^2 S_1^3 P_1 S_3^1 S_3^2 S_3^3 P_3 S_2^1 S_2^2 S_2^3 P_2$   
 282      ↓      ↓      ↓      ↓      ↓      ↓      ↓      ↓  
 283      If this is      Relevant      Not predictable  
 284      the prefix      future      from the prefix

285 Figure 4: Analysis on the modified sibling discovery task which requires adaptive future summaries.  
 286 **Left:** Convergence speed (mean (s.e.) over 3 random seeds) relative to NTP, where lower values  
 287 imply faster convergence. FSP-RevLM converges faster than NTP while FSP-BCE improves only  
 288 in the cases with few components. **Right:** Task setup illustration— given the prefix, only future  
 289 tokens in the highlighted component are informative. FSP-BCE, which summarizes all future tokens,  
 290 suffers from irrelevant information, whereas FSP-RevLM summarizes only the informative aspects.

291 Long handcrafted summaries often incorporate all future tokens, even though only a subset may  
 292 provide meaningful supervision signals, while the rest can introduce noise. This motivates the need  
 293 for an *adaptive* future summary. We illustrate this with modification of the sibling discovery task.  
 294 Figure 4 (right) depicts the setup, the model must generate sequences made of concatenated, inde-  
 295 pendent components, where each component lists its children nodes first, followed by their parent  
 296 (e.g., nodes  $S_1^1, S_2^1, S_3^1$  followed by parent  $P^1$ ).

297 Intuitively, the causal factorization implied by the DAG (parent followed by children) implies a  
 298 goal-conditioned approach: by conditioning on the parent, the model can easily capture the sibling  
 299 dependencies. Under NTP, the model estimates  $P_\theta(S_2^1 | S_1^1)$  without the parent, making sibling  
 300 relationships harder to learn and requiring more samples. Future prediction can help, when the model  
 301 predicts the parent from  $S_1^1$ , then the representation can incorporate the parent information. This  
 302 enables goal-conditioned planning, the model can predict  $S_2^1$  conditioned on both  $S_1^1$  and the parent,  
 303 allowing sample efficient learning of sibling relationships (see Nagarajan et al. (2025) for details).

304 However, not all future tokens are equally informative. As Figure 4 illustrates, future tokens from a  
 305 different component do not provide relevant signal for predicting  $S_2^1$ . Handcrafted summaries that  
 306 include all future tokens may therefore be affected by the irrelevant information, whereas learned  
 307 summaries remain robust, as the reverse language model learns representation that emphasize only  
 308 the predictive signals needed to infer the next token.

309 We verify this empirically by comparing FSP-BCE and FSP-RevLM in experiments with varying  
 310 number of total components. All models are pretrained from scratch with the GPT-Mini architecture  
 311 (details in Appendix B.2), and the inference task requires generating a coherent sequence (siblings  
 312 followed by parent for each component). At convergence, all models produce coherent sequences; to  
 313 quantify the learning speedup over NTP, we report the ratio of steps to convergence relative to NTP,  
 314 with lower values indicating faster learning. **Since all methods eventually reach perfect consistency**  
 315 **at convergence, time to convergence is a reliable metric for comparison.** Results in figure 4 (left)  
 316 shows that FSP-BCE improves over NTP only when the number of components is small, with gains  
 317 disappearing for more than six components. In contrast, FSP-RevLM consistently achieves faster  
 318 convergence across all component sizes, confirming the benefit of adaptive future summaries.

324 

## 4 EXPERIMENTS

325 

### 4.1 SETUP

326 We pretrain 3B- and 8B-parameter models on corpora of 250B and 1T tokens, respectively, covering  
 327 diverse domains. The majority of the data comes from DCLM-like sources and GitHub repositories,  
 328 supplemented by specialized material in mathematics, programming, and related areas. Models are  
 329 evaluated across a diverse set of benchmarks: ARC-Easy/Challenge (Clark et al., 2018) for general  
 330 reasoning, MBPP (Austin et al., 2021) and HumanEval+ (Liu et al., 2023) for code generation, and  
 331 GSM8K (Cobbe et al., 2021) and Math-500 (Hendrycks et al., 2021) for mathematical reasoning.  
 332 Details of the pretraining corpus and hyperparameters are provided in Appendix B.3.

333 We first benchmark our primary method, FSP-RevLM, against the baselines: next-token prediction  
 334 (NTP), standard multi-token prediction (MTP) (Gloeckle et al., 2024), and DeepSeek-MTP (DS-  
 335 MTP) (Liu et al., 2024). Further, a natural way to improve MTP for longer horizons is to add  
 336 multiple auxiliary heads, each predicting a token farther into the future, but this approach quickly  
 337 becomes impractical. We therefore constrain both MTP and DS-MTP to a single auxiliary head  
 338 predicting the immediate future token. This design choice keeps the comparison consistent and  
 339 aligned with the proposed FSP, since it uses a single auxiliary head.

340 Building on this unified single auxiliary head framework, we conduct an analysis of how MTP can  
 341 be enhanced by predicting richer future targets instead of the immediate future token. In addition  
 342 to predicting the learned future summary (FSP-RevLM), we compare handcrafted future summaries  
 343 over short- and long-range windows. This includes the proposed multi-hot future summary (FSP-  
 344 BCE) as a contributed baseline, and a random-token summary baseline (randomly sampling token  
 345 from future), in line with prior works (Thankaraj et al., 2025; Gerontopoulos et al., 2025).

346 **Note regarding experiment design.** All experiments are conducted under iso-data conditions,  
 347 meaning that all the methods are trained on identical datasets. For the proposed FSP-RevLM, this  
 348 implies that both the forward and reverse models are trained on the same data. In line with standard  
 349 practice in distillation, we do not perform iso-compute comparisons that include the teacher model’s  
 350 (ReverseLM) cost in the reported compute budget. In practical scenarios, the computational cost of  
 351 training the teacher model is typically amortized, hence it can be treated as a one-time overhead that  
 352 is excluded from comparisons of student models (Gemma et al., 2024; 2025).

353 **Note regarding FSP-RevLM implementation.** In our experiments with FSP-RevLM, the reverse  
 354 model is the same size as the forward model (and other baselines), and it is trained for the same  
 355 number of steps. As a result, FSP-RevLM roughly doubles the total compute cost compared to  
 356 standard NTP training. While FSP-RevLM increases training FLOPs, we believe this tradeoff is  
 357 reasonable in today’s compute-rich, data-limited scaling regime. The field has effectively hit the  
 358 data wall, whereas available compute continues to grow. Progress increasingly depends on using  
 359 this growing compute-per-token budget to extract more value from fixed datasets. In this context,  
 360 methods that deliver measurable gains without requiring additional data, even at higher compute  
 361 cost, are valuable.

362 

### 4.2 RESULTS

363 At the 8B scale (Table 1), future-summary supervision via the reverseLM (FSP-RevLM) consistently  
 364 improves the performance across different evaluation tasks. On ARC-Easy, FSP-RevLM (76.6%)  
 365 provides significant improvement over NTP (71.8%) and MTP (73.6%), and it also leads on ARC-  
 366 Challenge and MATH. For code generation, it achieves the highest score on MBPP and ties with  
 367 MTP on HumanEval+, showing that the benefits of predicting future summaries generalize across  
 368 both reasoning and program synthesis tasks. GSM8K is the one task where NTP (71.6%) holds a  
 369 lead, though FSP-RevLM (70.5%) still narrows the gap relative to MTP (67.8%).

370 At the 3B scale (Table 2), DeepSeek-MTP is a strong baseline and obtains better performance than  
 371 FSP-RevLM on most tasks, except math reasoning. More importantly, FSP-RevLM exhibits larger  
 372 relative improvements as scale increases from 3B to 8B parameters, and becomes more favourable  
 373 than DS-MTP. Further, note that even at the 3B scale, FSP-RevLM still beats MTP on ARC and  
 374 math reasoning tasks, and performs comparably on MBPP, suggesting that even at smaller scales,

Task	NTP	MTP	DS-MTP	FSP-RevLM
ARC-Easy	0.718 (0.000)	0.736 (0.000)	0.617 (0.003)	<b>0.766 (0.000)</b>
ARC-Challenge	0.531 (0.000)	0.552 (0.000)	0.426 (0.002)	<b>0.559 (0.000)</b>
GSM8K	<b>0.716 (0.003)</b>	0.678 (0.007)	0.704 (0.003)	0.705 (0.004)
MATH	0.342 (0.008)	0.309 (0.006)	0.335 (0.014)	<b>0.351 (0.017)</b>
MBPP	0.657 (0.004)	0.672 (0.008)	0.678 (0.006)	<b>0.683 (0.006)</b>
HumanEval+	0.478 (0.019)	<b>0.541 (0.011)</b>	0.526 (0.013)	<b>0.541 (0.009)</b>

Table 1: **Pretraining at 8B scale.** We benchmark the proposed FSP-RevLM approach against NTP, MTP, and DS-MTP. Results (mean  $\pm$  s.e. over 3 seeds) report pass@16 for code/math tasks and accuracy for ARC. FSP-RevLM achieves the strongest overall performance, with large gains over the baselines on ARC tasks and MATH, and competitive results with (DS) MTP on code benchmarks.

Task	NTP	MTP	DS-MTP	FSP-RevLM
ARC-Easy	0.263 (0.002)	0.272 (0.005)	<b>0.293 (0.000)</b>	0.277 (0.000)
ARC-Challenge	0.263 (0.001)	0.245 (0.002)	<b>0.274 (0.008)</b>	0.255 (0.000)
GSM8K	0.410 (0.003)	0.411 (0.001)	0.417 (0.003)	<b>0.436 (0.003)</b>
MATH	<b>0.213 (0.004)</b>	0.196 (0.009)	0.201 (0.004)	<b>0.212 (0.002)</b>
MBPP	0.521 (0.007)	0.526 (0.004)	<b>0.537 (0.007)</b>	0.524 (0.001)
HumanEval+	0.301 (0.009)	0.321 (0.015)	<b>0.348 (0.022)</b>	0.305 (0.006)

Table 2: **Pretraining at 3B scale.** We benchmark the proposed FSP-RevLM approach against NTP, MTP, and DS-MTP. Results (mean  $\pm$  s.e. over 3 seeds) report pass@16 for code/math tasks and accuracy for ARC. At this smaller scale, DS-MTP is a strong overall baseline, but FSP-RevLM outperforms it on math reasoning tasks, and also provides substantial gains over MTP on ARC and math reasoning tasks. Further, as we scale the approaches to 8B parameters, FSP-RevLM scales more favorably than DS-MTP, overtaking it on most tasks.

learning to predict future summaries may provide more effective auxiliary signal than immediate future token prediction with MTP.

#### 4.3 ANALYZING MTP WITH DIFFERENT FUTURE SUMMARIES

Table 3 presents our analysis of different future-summary strategies as auxiliary head targets at 8B scale. We focus on the standard MTP architecture, without comparing to DS-MTP as it modifies the input to auxiliary head, to isolate the effect of different future targets on the auxiliary head.

Our results show that random-token handcrafted future summaries perform worse than standard MTP with immediate future token prediction, and performance further degrades as the future window ( $\tau$ ) increases. In contrast, the proposed multi-hot or bag-of-words handcrafted future summaries yield meaningful improvements over MTP, especially on math reasoning tasks, with both shorter ( $\tau = 12$ ) and longer ( $\tau = 100$ ) future windows. For example, FSP-BCE with  $\tau = 12$  achieves 33.1% on MATH (+2.2 points) and 69.9% on GSM8K (+2.1 points), while even longer windows ( $\tau = 100$ ) further amplifies the performance on GSM8K (71.4%, +3.6 points).

Finally, our learned future summaries (FSP-RevLM) outperform MTP across all evaluation tasks, with especially pronounced gains on math reasoning: 35.1% on MATH (+4.2 points) and 70.5% on GSM8K (+3.5 points). Further analysis (Figure 5) for these math reasoning tasks shows that learned summaries promote greater output diversity across different pass@k settings, compared to vanilla MTP with immediate future token prediction.

In Appendix B.3 (Table 5), we replicate these findings at 3B scale, where both handcrafted and learned future summaries improve over vanilla MTP, again most prominently on math reasoning tasks. Additional ablations explore the effects of omitting reweighting in FSP-BCE and predicting learned summaries from deeper layers of the reverseLM (FSP-RevLM).

Method	MBPP	GSM8K	MATH	HumanEval+	ARC-Challenge	ARC-Easy
MTP	0.672 (0.008)	0.678 (0.007)	0.309 (0.006)	<b>0.541 (0.011)</b>	0.552 (0.000)	0.736 (0.000)
MTP-Skip $\tau:4$	0.658 (0.005)	0.639 (0.004)	0.277 (0.020)	0.508 (0.009)	0.494 (0.003)	0.722 (0.000)
MTP-Skip $\tau:12$	0.623 (0.002)	0.621 (0.005)	0.287 (0.018)	0.486 (0.010)	0.512 (0.000)	0.710 (0.003)
MTP-Skip $\tau:32$	0.611 (0.008)	0.598 (0.007)	0.271 (0.005)	0.459 (0.007)	0.379 (0.000)	0.564 (0.000)
FSP-BCE $\tau:12$	0.669 (0.005)	0.699 (0.006)	0.331 (0.016)	0.508 (0.005)	<b>0.562 (0.000)</b>	0.737 (0.000)
FSP-BCE $\tau:100$	0.671 (0.002)	<b>0.714 (0.009)</b>	0.331 (0.007)	0.500 (0.019)	0.459 (0.000)	0.662 (0.000)
FSP-RevLM	<b>0.683 (0.006)</b>	0.705 (0.004)	<b>0.351 (0.017)</b>	<b>0.541 (0.009)</b>	0.559 (0.000)	<b>0.766 (0.000)</b>

Table 3: **Analysis of future-summary strategies at 8B Scale.** We evaluate the effect of different future-summary prediction approaches against vanilla MTP. Results (mean  $\pm$  s.e. over 3 seeds) report pass@16 for code/math tasks and accuracy for ARC. Handcrafted multi-hot summaries (FSP-BCE) improve over standard MTP, especially on math reasoning (e.g., GSM8K and MATH), while learned summaries (FSP-RevLM) provide the largest gains across math reasoning and ARC tasks.

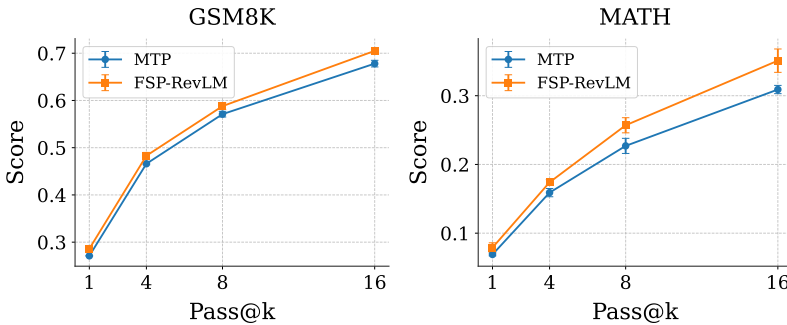


Figure 5: **Enhanced diversity through learned future summaries.** We compare standard MTP, which predicts the immediate future token, with FSP-RevLM, which enriches the auxiliary head target using learned future summaries. FSP-RevLM substantially increases output diversity compared to MTP on GSM8K and MATH benchmarks.

## 5 RELATED WORK

**Pitfalls of Next-Token Prediction (NTP).** While next-token prediction (NTP) is the standard loss for modern LLMs, its shortcomings are increasingly evident. The main issue is the mismatch between training (teacher forcing) and inference (autoregression): during training, the model sees ground-truth tokens, which encourages learning spurious correlations or “shortcuts” rather than the true data distribution. Bachmann & Nagarajan (2024) describe this as the “Clever Hans cheat”, where the model exploits trivial cues from the prefix and fails on lookahead tasks such as their path-star graph problem. Nagarajan et al. (2025) further show that NTP is data-inefficient for tasks requiring a “leap of thought,” such as Sibling Discovery. Our approach tackles these failures by providing a more robust, long-range training signal that discourages such shortcuts.

**Going Beyond Immediate Next Token.** Multi-Token Prediction (MTP) addresses limitations of Next Token Prediction (NTP) by using auxiliary heads to predict future tokens (Gloeckle et al., 2024). DeepSeek-V3 (Liu et al., 2024) modifies these auxiliary heads to allow slight teacher forcing, and recently Joint Token Prediction (Ahn et al., 2025) improves over DeepSeek-V3’s design of slight teacher forcing to predict the joint distribution of future tokens. But the key issue with all these approaches is that scaling the auxiliary heads for long-range dependencies is impractical. Recent work aims to improve efficiency and capture longer dependencies. Gerontopoulos et al. (2025) introduce register tokens, predicting tokens  $k$  steps ahead without architectural changes. Thankaraj et al. (2025) insert lookahead tokens containing future subsequences, while Liu et al. (2025) use a leap-based strategy to predict non-sequential future tokens. However, heuristically sampling random future tokens still poses the risk of missing informative long-range signals. Our FSP-RevLM

486 addresses this by *predicting a learned summary of the future*, such that it can extract meaningful  
 487 long-range information.  
 488

489 A relevant predecessor from the RNN literature that in principle avoids scaling auxiliary heads is  
 490 ProphetNet (Qi et al., 2020), which uses a shared self-attention mechanism together with relative  
 491 positional encodings to predict future n-grams without introducing separate heads. While this may  
 492 seem related to our bag-of-words summary (FSP-BCE), ProphetNet still supervises each future to-  
 493 ken individually and preserves positional order. In contrast, FSP-BCE operates on a summary vector  
 494 that discards positional information, and applies a binary cross-entropy objective over an unordered  
 495 future-token summary, yielding a fundamentally different training signal.  
 496

497 **Bidirectional models.** Leveraging reverse, or “right-to-left,” order during training has proven ef-  
 498 fective across several paradigms. The Belief State Transformer (BST) (Hu et al., 2024) uses dual  
 499 forward and backward encoders to predict the next token after a prefix and the previous token before  
 500 a suffix, encouraging a compact belief state, but does not explicitly reduce teacher forcing. Meet-  
 501 in-the-Middle (MiM) (Nguyen et al., 2023) jointly trains forward and backward models with shared  
 502 parameters, using an agreement regularizer to align their outputs. Reverse Training (Golovneva  
 503 et al., 2024) augments the dataset with reversed sequences to teach bidirectional dependencies and  
 504 mitigate the Reversal Curse (Berglund et al., 2023). Our FSP-RevLM similarly incorporates a re-  
 505 verse model but with a distinct goal: reducing reliance on teacher forcing. Trained on standard  
 506 left-to-right inputs, it aligns the forward model’s embeddings with the reverse model’s, effectively  
 507 distilling the reverse signal into the forward LM.  
 508

509 The most closely related work aimed at reducing teacher forcing is Twin Networks (Serdyuk et al.,  
 510 2017), which trains a reverse RNN and matches the forward hidden states to those of the reverse  
 511 model to encourage long-range future dependence. While similar at a high level, our contributions  
 512 go beyond the specific FSP-RevLM mechanism: we present a broader perspective in which future  
 513 summary prediction serves as a framework for understanding and designing pretraining objectives,  
 514 together with evidence showing when simpler approaches fail and why a learned summary coupled  
 515 with a reverse LM becomes necessary. Moreover, scaling this idea to Transformers is non-trivial.  
 516 Just as TwinNet anticipated aspects of our reverse component, earlier work also explored multiple  
 517 future tokens or parallel token blocks prediction from a given prefix (Tschannen et al., 2023; Monea  
 518 et al., 2023) well before Gloeckle et al. (2024), though without establishing MTP as a broadly  
 519 effective objective for large-scale Transformers. Gloeckle et al. (2024) deserve credit for identifying  
 520 a formulation that works in modern LLM training, and our results extend this line by showing that  
 521 both MTP and future-summary prediction can be cleanly integrated into Transformer pretraining  
 522 and scaled to yield robust gains.  
 523

524 Another somewhat related line is z-forcing (Goyal et al., 2017), which uses a reverse RNN to infer  
 525 latent variables that are then injected into the forward RNN to compute its hidden states. In contrast,  
 526 our reverse LM is not performing latent-variable inference; it is used solely to generate targets for an  
 527 auxiliary prediction head. Furthermore, unlike Z-forcing, our approach does not require the reverse  
 528 model at inference time—the reverse LM is purely a training-time component, whereas Z-forcing  
 529 depends on the reverse RNN during inference as well.  
 530

## 531 6 CONCLUSION

532 In this work, we highlighted a key limitation of existing multi-token prediction methods: the diffi-  
 533 culty of scaling auxiliary heads for long-horizon future prediction. Towards this, we proposed *Future*  
 534 *Summary Prediction* (FSP), a novel pretraining framework that shifts the auxiliary objective from  
 535 predicting specific future tokens to predicting a (learned) summary of the future. Experiments on 8B  
 536 models, using both hand-crafted and learned summaries, demonstrate that FSP delivers a stronger,  
 537 more robust training signal, improving over NTP and MTP on challenging reasoning and coding  
 538 tasks. Our findings indicate that focusing on abstract, predictable aspects of the future is a promis-  
 539 ing strategy for designing more efficient and effective pretraining objectives for next-generation  
 540 large language models.  
 541

540 REFERENCES  
541

542 Kwangjun Ahn, Alex Lamb, and John Langford. Efficient joint prediction of multiple future tokens.  
543 *arXiv preprint arXiv:2503.21801*, 2025.

544 Zeyuan Allen-Zhu and Yuanzhi Li. Physics of language models: Part 3.1, knowledge storage and  
545 extraction. *arXiv preprint arXiv:2309.14316*, 2023.

546 Jacob Austin, Augustus Odena, Maxwell Nye, Maarten Bosma, Henryk Michalewski, David Dohan,  
547 Ellen Jiang, Carrie Cai, Michael Terry, Quoc Le, et al. Program synthesis with large language  
548 models. *arXiv preprint arXiv:2108.07732*, 2021.

550 Zhangir Azerbayev, Hailey Schoelkopf, Keiran Paster, Marco Dos Santos, Stephen McAleer, Al-  
551 bert Q. Jiang, Jia Deng, Stella Biderman, and Sean Welleck. Llemma: An open language model  
552 for mathematics, 2023.

553 Gregor Bachmann and Vaishnavh Nagarajan. The pitfalls of next-token prediction. In *International  
554 Conference on Machine Learning*, pp. 2296–2318. PMLR, 2024.

555 Samy Bengio, Oriol Vinyals, Navdeep Jaitly, and Noam Shazeer. Scheduled sampling for sequence  
556 prediction with recurrent neural networks. *Advances in neural information processing systems*,  
557 28, 2015.

559 Lukas Berglund, Meg Tong, Max Kaufmann, Mikita Balesni, Asa Cooper Stickland, Tomasz Kor-  
560 bak, and Owain Evans. The reversal curse: Llms trained on “a is b” fail to learn “b is a”. *arXiv  
561 preprint arXiv:2309.12288*, 2023.

562 Tom Brown, Benjamin Mann, Nick Ryder, Melanie Subbiah, Jared D Kaplan, Prafulla Dhari-  
563 wal, Arvind Neelakantan, Pranav Shyam, Girish Sastry, Amanda Askell, Sandhini Agar-  
564 wal, Ariel Herbert-Voss, Gretchen Krueger, Tom Henighan, Rewon Child, Aditya Ramesh,  
565 Daniel Ziegler, Jeffrey Wu, Clemens Winter, Chris Hesse, Mark Chen, Eric Sigler, Mateusz  
566 Litwin, Scott Gray, Benjamin Chess, Jack Clark, Christopher Berner, Sam McCandlish, Alec  
567 Radford, Ilya Sutskever, and Dario Amodei. Language models are few-shot learners. In  
568 H. Larochelle, M. Ranzato, R. Hadsell, M.F. Balcan, and H. Lin (eds.), *Advances in Neu-  
569 ral Information Processing Systems*, volume 33, pp. 1877–1901. Curran Associates, Inc.,  
570 2020. URL [https://proceedings.neurips.cc/paper\\_files/paper/2020/  
571 file/1457c0d6bfc4967418bfb8ac142f64a-Paper.pdf](https://proceedings.neurips.cc/paper_files/paper/2020/file/1457c0d6bfc4967418bfb8ac142f64a-Paper.pdf).

572 Peter Clark, Isaac Cowhey, Oren Etzioni, Tushar Khot, Ashish Sabharwal, Carissa Schoenick, and  
573 Oyvind Tafjord. Think you have solved question answering? try arc, the ai2 reasoning challenge.  
574 *arXiv preprint arXiv:1803.05457*, 2018.

575 Karl Cobbe, Vineet Kosaraju, Mohammad Bavarian, Mark Chen, Heewoo Jun, Lukasz Kaiser,  
576 Matthias Plappert, Jerry Tworek, Jacob Hilton, Reiichiro Nakano, et al. Training verifiers to  
577 solve math word problems. *arXiv preprint arXiv:2110.14168*, 2021.

579 Leo Gao, Stella Biderman, Sid Black, Laurence Golding, Travis Hoppe, Charles Foster, Jason  
580 Phang, Horace He, Anish Thite, Noa Nabeshima, Shawn Presser, and Connor Leahy. The Pile:  
581 An 800gb dataset of diverse text for language modeling. *arXiv preprint arXiv:2101.00027*, 2020.

583 Team Gemma, Morgane Riviere, Shreya Pathak, Pier Giuseppe Sessa, Cassidy Hardin, Surya Bhu-  
584 patiraju, Léonard Hussonot, Thomas Mesnard, Bobak Shahriari, Alexandre Ramé, et al. Gemma  
585 2: Improving open language models at a practical size. *arXiv preprint arXiv:2408.00118*, 2024.

586 Team Gemma, Aishwarya Kamath, Johan Ferret, Shreya Pathak, Nino Vieillard, Ramona Merhej,  
587 Sarah Perrin, Tatiana Matejovicova, Alexandre Ramé, Morgane Rivière, et al. Gemma 3 technical  
588 report. *arXiv preprint arXiv:2503.19786*, 2025.

589 Anastasios Gerontopoulos, Spyros Gidaris, and Nikos Komodakis. Multi-token prediction needs  
590 registers, 2025. URL <https://arxiv.org/abs/2505.10518>.

592 Fabian Gloeckle, Badr Youbi Idrissi, Baptiste Rozière, David Lopez-Paz, and Gabriel Synnaeve.  
593 Better & faster large language models via multi-token prediction. In *Proceedings of the 41st  
International Conference on Machine Learning*, pp. 15706–15734, 2024.

594 Olga Golovneva, Zeyuan Allen-Zhu, Jason Weston, and Sainbayar Sukhbaatar. Reverse training to  
 595 nurse the reversal curse. *arXiv preprint arXiv:2403.13799*, 2024.

596

597 Anirudh Goyal, Alessandro Sordoni, Marc-Alexandre Côté, Nan Rosemary Ke, and Yoshua Bengio.  
 598 Z-forcing: Training stochastic recurrent networks. *Advances in neural information processing  
 599 systems*, 30, 2017.

600 Dan Hendrycks, Collin Burns, Saurav Kadavath, Akul Arora, Steven Basart, Eric Tang, Dawn Song,  
 601 and Jacob Steinhardt. Measuring mathematical problem solving with the math dataset. *arXiv  
 602 preprint arXiv:2103.03874*, 2021.

603

604 Edward S Hu, Kwangjun Ahn, Qinghua Liu, Haoran Xu, Manan Tomar, Ada Langford, Dinesh  
 605 Jayaraman, Alex Lamb, and John Langford. The belief state transformer. *arXiv preprint  
 606 arXiv:2410.23506*, 2024.

607 Jared Kaplan, Sam McCandlish, T. J. Henighan, Tom B. Brown, Benjamin Chess, Rewon Child,  
 608 Scott Gray, Alec Radford, Jeff Wu, and Dario Amodei. Scaling laws for neural language  
 609 models. *ArXiv*, abs/2001.08361, 2020. URL <https://api.semanticscholar.org/CorpusID:210861095>.

610

611 Jeffrey Li, Alex Fang, et al. Datacomp-lm: In search of the next generation of training sets for  
 612 language models, 2025. URL <https://arxiv.org/abs/2406.11794>.

613

614 Wang Ling, Dani Yogatama, Chris Dyer, and Phil Blunsom. Program induction by rationale  
 615 generation : Learning to solve and explain algebraic word problems, 2017. URL <https://arxiv.org/abs/1705.04146>.

616

617 Aixin Liu, Bei Feng, Bing Xue, Bingxuan Wang, Bochao Wu, Chengda Lu, Chenggang Zhao,  
 618 Chengqi Deng, Chenyu Zhang, Chong Ruan, et al. Deepseek-v3 technical report. *arXiv preprint  
 619 arXiv:2412.19437*, 2024.

620

621 Jiawei Liu, Chunqiu Steven Xia, Yuyao Wang, and Lingming Zhang. Is your code generated by chat-  
 622 gpt really correct? rigorous evaluation of large language models for code generation. *Advances  
 623 in Neural Information Processing Systems*, 36:21558–21572, 2023.

624

625 Xiaohao Liu, Xiaobo Xia, Weixiang Zhao, Manyi Zhang, Xianzhi Yu, Xiu Su, Shuo Yang, See-  
 626 Kiong Ng, and Tat-Seng Chua. L-mtp: Leap multi-token prediction beyond adjacent context for  
 627 large language models. *arXiv preprint arXiv:2505.17505*, 2025.

628

629 Anton Lozhkov, Loubna Ben Allal, Leandro von Werra, and Thomas Wolf. Fineweb-edu: the finest  
 630 collection of educational content, 2024. URL <https://huggingface.co/datasets/HuggingFaceFW/fineweb-edu>.

631

632 Giovanni Monea, Armand Joulin, and Edouard Grave. Pass: Parallel speculative sampling. *arXiv  
 633 preprint arXiv:2311.13581*, 2023.

634

635 Vaishnavh Nagarajan, Chen Henry Wu, Charles Ding, and Aditi Raghunathan. Roll the dice &  
 636 look before you leap: Going beyond the creative limits of next-token prediction. In *Forty-second  
 637 International Conference on Machine Learning*. PMLR, 2025.

638

639 neogithub. Github code dataset, 2022. <https://huggingface.co/datasets/codeparrot/github-code>.

640

641 Anh Nguyen, Nikos Karampatziakis, and Weizhu Chen. Meet in the middle: A new pre-training  
 642 paradigm. *Advances in Neural Information Processing Systems*, 36:5079–5091, 2023.

643

644 Pinelopi Papalampidi, Kris Cao, and Tomas Kociský. Towards coherent and consistent use of entities  
 645 in narrative generation. In *International Conference on Machine Learning*, pp. 17278–17294.  
 646 PMLR, 2022.

647

648 Mohammad Pezeshki, Oumar Kaba, Yoshua Bengio, Aaron C Courville, Doina Precup, and Guil-  
 649 laume Lajoie. Gradient starvation: A learning proclivity in neural networks. *Advances in Neural  
 650 Information Processing Systems*, 34:1256–1272, 2021.

648 Weizhen Qi, Yu Yan, Yeyun Gong, Dayiheng Liu, Nan Duan, Jiusheng Chen, Ruofei Zhang, and  
649 Ming Zhou. Prophetnet: Predicting future n-gram for sequence-to-sequence pre-training. *arXiv*  
650 *preprint arXiv:2001.04063*, 2020.

651

652 David Saxton, Edward Grefenstette, Felix Hill, and Pushmeet Kohli. Analysing mathematical rea-  
653 soning abilities of neural models, 2019. URL <https://arxiv.org/abs/1904.01557>.

654

655 Dmitriy Serdyuk, Nan Rosemary Ke, Alessandro Sordoni, Adam Trischler, Chris Pal, and Yoshua  
656 Bengio. Twin networks: Matching the future for sequence generation. *arXiv preprint*  
657 *arXiv:1708.06742*, 2017.

658

659 Ilya Sutskever. Sequence to sequence learning with neural networks: What a decade. *NeurIPS 2024*  
660 Test-of-Time Talk (YouTube video), 2024. URL <https://www.youtube.com/watch?v=1yvBqashLzs>. Presented at NeurIPS 2024, Vancouver, Canada.

661

662 Abitha Thankaraj, Yiding Jiang, J. Zico Kolter, and Yonatan Bisk. Looking beyond the next token,  
663 2025. URL <https://arxiv.org/abs/2504.11336>.

664

665 Michael Tschannen, Manoj Kumar, Andreas Steiner, Xiaohua Zhai, Neil Houlsby, and Lucas Beyer.  
666 Image captioners are scalable vision learners too. *Advances in Neural Information Processing*  
667 *Systems*, 36:46830–46855, 2023.

668

669 An Yang, Anfeng Li, Baosong Yang, Beichen Zhang, Binyuan Hui, Bo Zheng, Bowen Yu,  
670 Chang Gao, Chengan Huang, Chenxu Lv, et al. Qwen3 technical report. *arXiv preprint*  
671 *arXiv:2505.09388*, 2025.

672

673 Weizhe Yuan, Jane Yu, Song Jiang, Karthik Padthe, Yang Li, Dong Wang, Ilia Kulikov, Kyunghyun  
674 Cho, Yuandong Tian, Jason E Weston, and Xian Li. Naturalreasoning: Reasoning in the wild with  
675 2.8m challenging questions, 2025. URL <https://arxiv.org/abs/2502.13124>.

676

677

678

679

680

681

682

683

684

685

686

687

688

689

690

691

692

693

694

695

696

697

698

699

700

701

702  
703  

## A ADDITIONAL MTP VARIANTS

704  
705  
In Section 2, we discussed MTP and the proposed future summary prediction to address a major  
706  
limitation in MTP. We summarize other variants proposed in the literature and their limitations here.  
707708  
709  
**DeepSeek (DS) MTP.** Another popular variant for MTP was proposed in DeepSeek (Liu  
710  
et al., 2024), where we condition the auxiliary head  $f'_{h_k}$  with full prefix  $x_{\leq t+k-1}$  to pre-  
711  
dict the future tokens  $x_{t+k}$ , but with reduced teacher forcing from the “auxiliary” tokens  
 $\{x_{t+1}, x_{t+2}, \dots, x_{\leq t+k-1}\}$ .  
712

713  
$$L_{\text{DSMTP}}(X, P_\theta) = -\mathbb{E}_{x \sim \mathbb{P}_X} \left[ \sum_{t=1}^{T-1} \sum_{k=1}^{\tau} \mathbf{1}[t+k \leq T] \log P_\theta(x_{t+k} | x_{\leq t+k-1}) \right]. \quad (14)$$
  
714

715  
The parameterization is:  
716

717  
$$\begin{aligned} P_\theta(x_{t+1} | x_{\leq t}) &= \text{softmax}\left(f_u \circ f_h \circ f_s(x_{\leq t})\right), \\ P_\theta(x_{t+k} | x_{\leq t+k-1}) &= \text{softmax}\left(f_u \circ f'_{h_k}\left(f_s(x_{\leq t}), x_{t+1}, \dots, x_{t+k-1}\right)\right), \quad \forall k > 1. \end{aligned} \quad (15)$$
  
718  
719  
720

721  
Here, the auxiliary (future) tokens  $(x_{t+1}, \dots, x_{t+k-1})$  are injected directly into the auxiliary heads,  
722  
bypassing the backbone, which reduces teacher forcing compared to standard NTP.  
723724  
However, this approach suffers from the same short-horizon limitation as MTP: predicting multiple  
725  
future steps would require adding separate auxiliary heads for each token, which quickly becomes  
726  
impractical and limits scalability to long future sequences.  
727728  
**TRELAWNEY.** In this work, we emphasized that standard MTP and DS-MTP often fail to cap-  
729  
ture the most informative future tokens, as both primarily focus on predicting the immediate next  
730  
tokens via the auxiliary head. The TRELAWNEY approach of Thankaraj et al. (2025) adopts a  
731  
complementary strategy: rather than altering the model architecture, it augments the training data  
732  
by inserting a window of future tokens, bounded by special markers. This encourages the model to  
733  
predict an the sampled block of future tokens, thereby reducing reliance on teacher forcing. More-  
734  
over, TRELAWNEY allows random subsequences to be sampled from the future, with the goal of  
735  
exposing the model to a richer and more informative signal than what is available in the immediate  
736  
next few steps. However, this heuristic random sampling can still fail to capture critical information  
737  
from tokens far in the future, limiting its robustness for long-horizon planning tasks.  
738  
739  
740  
741  
742  
743  
744  
745  
746  
747  
748  
749  
750  
751  
752  
753  
754  
755

756 **B EXPERIMENTS**  
757758 **B.1 PATH-STAR GRAPH**  
759760 **Experiment Setup.** We adopt the dataset generation procedure from the official code repository<sup>1</sup>  
761 of Bachmann & Nagarajan (2024). Specifically, we construct a set of 50 distinct nodes and generate  
762 multiple instances of path-star graph sequences by randomly sampling nodes from this set. The  
763 training set consists of  $n_{\text{train}} = 200,000$  sequences, and evaluation is performed on  $n_{\text{test}} = 20,000$   
764 sequences.765 For modeling, we employ the GPT-Mini architecture with the following configuration:  
766767 

- Total Layers: 12
- Embedding Dimension: 384
- Total Attention Heads: 6
- MLP expansion factor: 4

  
772

773 We summarize the other relevant hyperparameters below.

774 

- Learning Rate:  $3e - 4$
- Batch Size: 256
- Weight Decay:  $1e - 2$
- Total Epochs: 500
- Gradient Norm Clipping: 1.0

  
780781 **Experiment with multiple auxiliary heads in MTP.** A naive approach to incorporate longer-  
782 term future dependencies in MTP is by increasing the number of auxiliary heads. Table 4 reports the  
783 results: adding more auxiliary heads improves performance on  $G(2, 6)$ , due to reduced teacher for-  
784 cing. However, simply scaling the number of auxiliary heads is not a practical solution for modeling  
785 long-range dependencies, as shown by the poor performance on the longer path graph  $G(2, 8)$ .  
786787 

Method	G(2,6)	G(2,8)
NTP	0.45 (0.01)	0.45 (0.03)
MTP	0.66 (0.17)	0.15 (0.15)
MTP (aux heads: 2)	0.79 (0.13)	0.28 (0.11)
MTP (aux heads: 3)	0.90 (0.10)	0.38 (0.09)
MTP (aux heads: 4)	0.90 (0.10)	0.20 (0.12)
BCE	1.00 (0.00)	1.00 (0.00)

  
794795 **Table 4: Analyzing the performance of MTP on path-star graphs with an increasing number of aux-  
796 illiary heads.** Augmenting MTP with additional auxiliary heads improves performance on  $G(2, 6)$ ,  
797 but practical limits exist: even with four auxiliary heads, MTP fails to solve the longer path graph  
798  $G(2, 8)$ .  
799800 **B.2 SIBLING DISCOVERY**  
801802 **Experiment Setup.** We build on the dataset generation procedure from the official code reposi-  
803 tory<sup>2</sup> of Nagarajan et al. (2025). While the original sibling discovery task presents sequences from  
804 a single component, we modify the setup by concatenating sequences from multiple components.  
805 Each component  $i$  is defined by a unique parent  $P^i$  and three child nodes  $S_1^i, S_2^i, S_3^i$ . The support  
806 of each conditional distribution  $P(S^i | P^i)$  is disjoint across children—i.e., each child  $S^i$  can take  
807  $N$  possible values, and these sets of values are non-overlapping across children. As a result, with  $K$   
808 components, the total number of distinct child value combinations is  $N^{3K}$ . In our experiments, we  
809<sup>1</sup><https://github.com/gregorbachmann/Next-Token-Failures/><sup>2</sup><https://github.com/chenwu98/algorithmic-creativity>

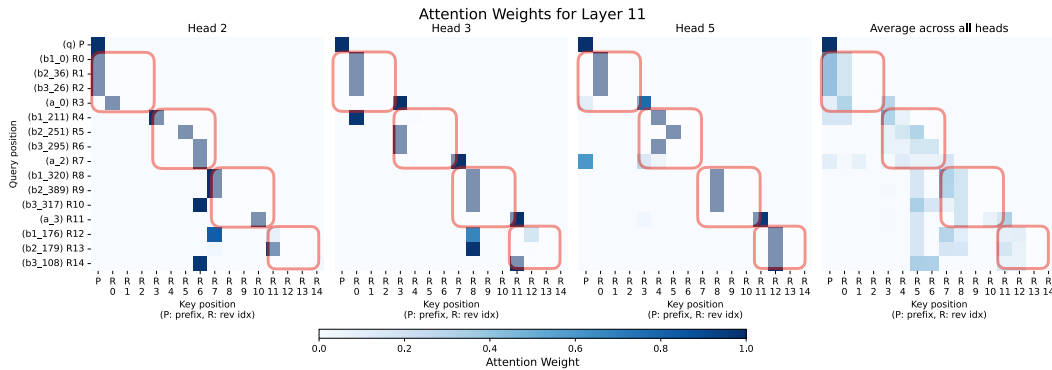
810 vary the number of components  $K \in 2, 4, 6, 8, 10$  while fixing  $N = 100$ . For training, we randomly  
 811 sample child values for each component to construct  $n_{\text{train}} = 20,000$  sequences, and evaluate on  
 812  $n_{\text{test}} = 3,000$  sequences.  
 813

814 We use the GPT-Mini architecture with the following specifications.  
 815

- Total Layers: 12
- Embedding Dimension: 384
- Total Attention Heads: 6
- MLP expansion factor: 4

821 We summarize the other relevant hyperparameters below.  
 822

- Learning Rate:  $3e - 4$
- Batch Size: 256
- Weight Decay:  $1e - 2$
- Total Epochs: 150



850 Figure 6: Each subplot corresponds to a different attention head. Red squares highlight queries  
 851 belonging to a particular component, showing that they attend predominantly to keys within the  
 852 same component, forming a subgroup-wise pattern. While the average across heads shows some  
 853 cross-component diffusion, several heads exhibit clean intra-component attention, indicating that the  
 854 reverse model preserves the structural organization of the future input rather than mixing information  
 855 across unrelated parts of the sequence.  
 856

857 **Additional Experiment: Interpretability of attention weights from RevLM.** Interpreting the  
 858 learned future summaries is crucial for understanding how RevLM captures information from future  
 859 context. For the sibling-discovery experiment (Section 3.2), we conducted a preliminary analysis  
 860 using attention weights from the final layer, which directly contribute to the future-summary repre-  
 861 sentation. We observe that queries associated with a particular component in the sequence attend  
 862 predominantly to keys from the same component, indicating limited cross-component interaction.  
 863 While the average across heads shows some diffusion of attention beyond component boundaries,  
 864 three individual heads exhibit a clear subgroup-wise structure without such leakage. This suggests

864 that the learned future summaries preserve the informative structure of the future input by prioritizing  
 865 intra-component tokens. Prior work shows that hidden states of LLMs naturally encode detailed  
 866 information about surrounding tokens (see Section 5 of Physics of LLMs (Allen-Zhu & Li, 2023)),  
 867 supporting the intuition that reverse-direction representations can capture meaningful long-range  
 868 patterns. Extending this analysis with additional interpretability tools, such as linear probing and  
 869 activation patching, remains a promising direction for future work.  
 870

### 871 B.3 REAL WORLD PRETRAINING

872 **Pretraining dataset composition.** Our pretraining corpus is constructed to cover a wide range  
 873 of domains, aiming to equip models with both broad knowledge and strong reasoning ability.  
 874 The bulk of the data is drawn from a DCLM-style mixture (Li et al., 2025) and large-scale code  
 875 sources such as GitHub (neogithub, 2022). To strengthen performance on more specialized skills,  
 876 we further supplement with mathematics and scientific data, including the DeepMind Mathematics  
 877 dataset (Saxton et al., 2019), Proof Pile 2 (ArXiv, OpenWebMath, Algebraic Stack) (Azerbayev  
 878 et al., 2023), and Stack Exchange from the Pile (Gao et al., 2020). Additional curated resources in-  
 879 clude FineWeb-Edu (Lozhkov et al., 2024), the Natural Reasoning Dataset (Yuan et al., 2025), and  
 880 AQuA (Ling et al., 2017). Together, this mixture balances large-scale general text with carefully  
 881 chosen reasoning-focused datasets.  
 882

883 **Pretraining hyperparameters.** All the models were trained using NVIDIA H200 GPUs. We train  
 884 models using a cosine learning rate scheduler, with an initial learning rate of  $3 \times 10^{-3}$  for 3B models  
 885 and  $3 \times 10^{-4}$  for 8B models. We provide details regarding the other hyperparameters below.

- 886 • **3B Models**

- 887 – Batch Size (per GPU): 16
- 888 – Total GPUs: 128
- 889 – Sequence Length: 2048
- 890 – Total Steps: 60k

- 891 • **8B Models**

- 892 – Batch Size (per GPU): 2
- 893 – Total GPUs: 256
- 894 – Sequence Length: 8192
- 895 – Total Steps: 240k

896 **Evaluation Metrics.** We report accuracy for ARC and pass@k for code and math reasoning tasks,  
 897 with mean and standard error computed over 3 random seeds. For pass@k, we evaluate each method  
 898 across a range of temperature values (0, 0.1, 0.2, . . . , 0.9, 1.0) and report the results corresponding  
 899 to the temperature that yields the best performance for each method and task. Note that, in all  
 900 cases, the auxiliary head is used only during training, and methods are evaluated via their next-token  
 901 prediction heads at test time.  
 902

918  
 919 **Additional Experiment: Analysis of future summaries (3B).** Table 5 presents our analysis of  
 920 different future-summary strategies as auxiliary head targets at the 3B scale. Similar to the 8B  
 921 case, we focus on the standard MTP architecture, without comparing to DS-MTP since it modi-  
 922 fies the input to the auxiliary head, allowing us to isolate the effect of different future targets. Our  
 923 findings are similar: random-skip handcrafted summaries underperform relative to MTP, while the  
 924 proposed multi-hot/bag-of-words approaches perform well. In our experiments, we observed con-  
 925 sistent improvement over MTP with the proposed handcrafted summaries (FSP-BCE) on both Math  
 926 and GSM8k tasks, across the 3B and 8B model scales. For the 3B ablation, we tested removing  
 927 tf-idf reweighting as well and found that, in most cases, it did not provide benefits, which led us to  
 928 keep the tf-idf reweighting for our 8B experiments. The only exceptions where no tf-idf reweighting  
 929 performed better were GSM8k at  $\tau = 12$  and HumanEval+ at  $\tau = 10$ . Additionally, we exper-  
 930 imented with using deeper layers at the 3B scale and found that the last layer performed better on  
 931 ARC Challenge and ARC Easy, though it was slightly worse on MBPP and Math. Based on these  
 932 findings, we chose to use the last layer for our 8B-scale experiments.  
 933

Method	MBPP	GSM8K	MATH	HumanEval+	ARC-Challenge	ARC-Easy
MTP	0.526 (0.004)	0.411 (0.001)	0.196 (0.009)	<b>0.321</b> (0.015)	0.245 (0.002)	0.272 (0.005)
MTP-Skip $\tau:4$	0.519 (0.004)	0.368 (0.007)	0.181 (0.005)	0.309 (0.004)	0.241 (0.000)	0.282 (0.000)
MTP-Skip $\tau:12$	0.485 (0.011)	0.354 (0.005)	0.177 (0.006)	0.287 (0.009)	0.264 (0.008)	0.262 (0.000)
MTP-Skip $\tau: 32$	0.467 (0.007)	0.354 (0.003)	0.189 (0.004)	0.278 (0.017)	0.243 (0.000)	0.240 (0.003)
FSP-BCE $\tau:12$ , no tf-idf	0.518 (0.006)	0.431 (0.004)	0.201 (0.009)	0.301 (0.009)	0.250 (0.000)	0.251 (0.000)
FSP-BCE $\tau:12$	0.521 (0.005)	0.419 (0.003)	0.204 (0.002)	0.305 (0.012)	0.254 (0.000)	0.262 (0.004)
FSP-BCE $\tau:100$ , no tf-idf	0.512 (0.007)	0.416 (0.005)	0.203 (0.008)	0.309 (0.004)	0.228 (0.003)	0.238 (0.000)
FSP-BCE $\tau:100$	0.524 (0.004)	0.417 (0.004)	0.209 (0.003)	0.293 (0.012)	0.254 (0.006)	0.262 (0.000)
FSP-RevLM depth: 2	<b>0.528 (0.004)</b>	0.428 (0.003)	<b>0.217 (0.006)</b>	0.305 (0.013)	0.243 (0.007)	0.265 (0.000)
FSP-RevLM	0.524 (0.001)	<b>0.436 (0.003)</b>	0.212 (0.002)	0.305 (0.006)	<b>0.255 (0.000)</b>	<b>0.277 (0.000)</b>

934  
 935 **Table 5: Analysis of future summaries at 3B Scale.** We evaluate the effect of different future-  
 936 summary prediction approaches against vanilla MTP. Results (mean  $\pm$  s.e. over 3 seeds) report  
 937 pass@16 for code/math tasks and accuracy for ARC. Handcrafted multi-hot summaries (FSP-BCE)  
 938 improve over standard MTP, especially on math reasoning (e.g., GSM8K and MATH), while learned  
 939 summaries (FSP-RevLM) provide the largest gains across math reasoning and ARC tasks.  
 940

941  
 942  
 943  
 944  
 945  
 946  
 947  
 948  
 949  
 950  
 951  
 952  
 953  
 954  
 955  
 956  
 957  
 958  
 959  
 960  
 961  
 962  
 963  
 964  
 965  
 966  
 967  
 968  
 969  
 970  
 971